

Refractory titanium nitride two-dimensional structures with extremely narrow surface lattice resonances at telecommunication wavelengths

Vadim I. Zakomirnyi, Ilia L. Rasskazov, Valeriy S. Gerasimov, Alexander E. Ershov, Sergey P. Polyutov, and Sergei V. Karpov

Citation: *Appl. Phys. Lett.* **111**, 123107 (2017); doi: 10.1063/1.5000726

View online: <http://dx.doi.org/10.1063/1.5000726>

View Table of Contents: <http://aip.scitation.org/toc/apl/111/12>

Published by the [American Institute of Physics](#)

A banner for SciLight featuring a dark blue background with a network of glowing yellow nodes and blue lines. The text 'SciLight' is prominently displayed in white and yellow.

SciLight

Sharp, quick summaries **illuminating**
the latest physics research

Sign up for **FREE!**

The logo for AIP Publishing, consisting of the letters 'AIP' in a bold, sans-serif font above the word 'Publishing' in a smaller font, all contained within a white square with a thin black border.

AIP
Publishing

Refractory titanium nitride two-dimensional structures with extremely narrow surface lattice resonances at telecommunication wavelengths

Vadim I. Zakomirnyi,^{1,2} Iliia L. Rasskazov,^{3,a)} Valeriy S. Gerasimov,¹
 Alexander E. Ershov,^{1,4,5} Sergey P. Polyutov,¹ and Sergei V. Karpov^{1,5,6}

¹*Institute of Nanotechnology, Spectroscopy and Quantum Chemistry, Siberian Federal University, Krasnoyarsk 660041, Russia*

²*Division of Theoretical Chemistry and Biology, School of Biotechnology, KTH Royal Institute of Technology, 10691 Stockholm, Sweden*

³*Beckman Institute for Advanced Science and Technology, University of Illinois at Urbana-Champaign, Urbana, Illinois 61801, USA*

⁴*Institute of Computational Modeling, Federal Research Center KSC SB RAS, 660036, Krasnoyarsk, Russia*

⁵*Siberian State University of Science and Technology, Krasnoyarsk 660014, Russia*

⁶*L. V. Kirensky Institute of Physics, Federal Research Center KSC SB RAS, 660036 Krasnoyarsk, Russia*

(Received 17 August 2017; accepted 13 September 2017; published online 22 September 2017)

Regular arrays of plasmonic nanoparticles have brought significant attention over the last decade due to their ability to support localized surface plasmons (LSPs) and exhibit diffractive grating behavior simultaneously. For a specific set of parameters (i.e., period, particle shape, size, and material), it is possible to generate super-narrow surface lattice resonances (SLRs) that are caused by interference of the LSP and the grating Rayleigh anomaly. In this letter, we propose plasmonic structures based on regular 2D arrays of TiN nanodisks to generate high- Q SLRs in an important telecommunication range, which is quite difficult to achieve with conventional plasmonic materials. The position of the SLR peak can be tailored within the whole telecommunication bandwidth (from $\approx 1.26 \mu\text{m}$ to $\approx 1.62 \mu\text{m}$) by varying the lattice period, while the Q -factor is controlled by changing nanodisk sizes. We show that the Q -factor of SLRs can reach a value of 2×10^3 , which is the highest reported Q -factor for SLRs at telecommunication wavelengths so far. Tunability of optical properties, refractory behavior, and low-cost fabrication of TiN nanoparticles paves the way for manufacturing cheap nanostructures with extremely stable and adjustable electromagnetic response at telecommunication wavelengths for a large number of applications. *Published by AIP Publishing.* [<http://dx.doi.org/10.1063/1.5000726>]

Regular arrays of plasmonic nanoparticles exhibit a unique feature: the existence of collective modes that originate from strong coupling between localized surface plasmons (LSPs) and the grating Rayleigh anomalies. Such strong hybrid coupling gives rise to narrow surface lattice resonances (SLRs) which tremendously outperform quality factor Q of LSP. SLRs have attracted significant attention during the last decade starting from pioneering theoretical^{1–3} and experimental^{4–6} studies with promising applications in vibrational spectroscopy,⁷ ultranarrow band absorption,⁸ sensing,^{9,10} lasers,¹¹ and fluorescence enhancement.^{12,13} SLRs were studied in a wide variety of periodic nanostructures with different kinds of unit cells: single¹⁴ or double-stack¹⁵ nanodisks, core-shell cylinders,¹⁶ nanoparticle dimers,^{17,18} nanorings,¹⁹ split-ring resonators,²⁰ oligomers,²¹ and more complex configurations.^{22–25}

Nowadays, much attention is focused on gratings made of classic plasmonic materials (Au and Ag) with the LSP peak of individual particles lying in the visible or near-infrared (NIR) regions. The position of the SLR peak in such structures is strictly limited to visible and NIR since the strongest coupling between LSP and Rayleigh anomaly takes place at certain wavelength.^{1,2,14} The SLR peak is red-shifted compared to the LSP peak and slightly blue-shifted compared to the position of Rayleigh anomaly. The telecommunication

wavelength range, which is important for a large number of applications and especially for hybrid nanophotonics interconnects,²⁶ remains almost unreachable for SLRs with conventional plasmonic materials. Utilization of non-spherical or non-homogeneous particles may lead to a significant shift of LSP to longer wavelengths; however, it is quite complicated to cover telecommunication bandwidth with classic plasmonic materials keeping reliable values of the SLR Q -factor. Although regular Au nanostructures on metal-dielectric substrates possess SLRs at telecommunication wavelengths with high quality factors^{27,28} (up to $Q \approx 300$), such performance is notably poorer than the one recently reported for SLRs in the visible range for 2D arrays of Au nanodisks¹⁴ ($Q > 1000$).

Here, we propose to enhance SLRs within the telecommunication wavelength range by utilizing so-called alternative plasmonic materials.²⁹ Among numerous possible choices, titanium nitride (TiN) has been considered as the most promising candidate to reduce the supremacy of gold and silver^{30–32} in a number of applications.^{33–35} Low-cost large-area fabrication of TiN nanostructures,³⁶ full CMOS-compatibility,³⁷ refractory behavior,^{38,39} and wide tunability of optical and structural properties^{30,40} make TiN an attractive alternative plasmonic material. However, what is really important, the LSP peak of a single TiN nanoparticle lies in the NIR region,³⁰ which is crucial for tailoring the position of the SLR peak beyond the visible range. The last feature

^{a)}Electronic mail: iliar@illinois.edu

represents the cornerstone of this work in which we provide the concept of $2D$ regular structures from TiN nanodisks with high- Q factor SLRs at telecom wavelengths.

It is a well known fact that optical properties of TiN as a non-stoichiometric material strongly depend on its synthesis conditions. TiN thin films exhibit color variations⁴¹ and even notable metallic luster³⁰ with changing composition and lattice parameters which can be controlled, for example, by varying the temperature of its deposition. Thus, for a particular set of deposition parameters, it is possible to enhance the plasmonic behavior of TiN structures.⁴⁰ Therefore, to provide a comparative analysis of SLR performance and to reveal the importance of tunability of TiN optical properties, we have chosen two different datasets for TiN dielectric permittivity ϵ : (i) recently acquired temperature- and size-dependent data for plasmonic-like TiN *thin films* from Ref. 42 and (ii) widely used tabulated data for *bulk* TiN at room temperature from Ref. 43.

Before discussing SLRs on regular arrays, it is insightful to investigate plasmonic properties of a single TiN nanoparticle. Although it is obvious that the shape of a nanoparticle is an important factor which definitely affects the Q -factor of SLR, we restrict ourselves to nanodisks. A nanodisk is a quite easy-to-fabricate shape from an experimental point of view and one of the most reliable shapes for high- Q SLRs.¹⁴ We consider nanodisks with three different diameters d : 160, 180 and 200 nm and fix height to $h = d/2$ for all cases. For dataset from Ref. 42, dielectric permittivity for each particular height h of nanodisk has been calculated by linear interpolation of $\epsilon(h)$. Normal plane wave incidence with polarization of the electric field perpendicular to the symmetry axis of a nanodisk was used in simulations, as shown in Fig. 1(c). Extinction cross section σ_{ext} of a nanodisk was calculated with commercial Lumerical finite-difference time-domain (FDTD) software package.⁴⁴

Figures 1(a) and 1(b) clearly show that the LSP peak of a single nanodisk lies from $\lambda \approx 950$ nm to $\lambda \approx 1050$ nm, depending on its size. It is quite difficult to tailor the LSP peak to this wavelength region and to maintain its quality factor with homogeneous nanoparticles made of conventional plasmonic materials. Comparison of σ_{ext} calculated with two different datasets for ϵ shows that tunability of TiN optical properties makes it possible to increase noticeably LSP quality factor of a single nanodisk, which is preferable for enhancing LSP-Rayleigh anomaly hybridization.

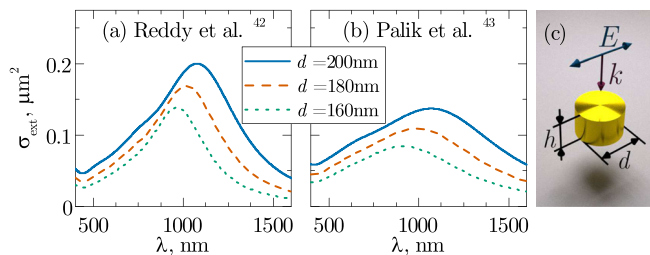


FIG. 1. (a) and (b) Extinction spectra of a single TiN nanodisk with a given diameter d and height $h = d/2$. Nanodisk is embedded in homogeneous medium with $n_m = 1.5$. Spectra are provided for two different datasets for ϵ of TiN: Refs. 42 and 43. (c) Schematic representation of a single TiN nanodisk illumination.

Then, we continue with the spectral properties of $2D$ regular arrays of TiN nanodisks, the schematic representation of which is depicted in Fig. 2. The period D of the lattice is varied to match the $(\pm 1, 0)$ and $(0, \pm 1)$ Rayleigh anomalies,⁴⁵ whose positions for the case of normal incidence and homogeneous surrounding with refractive index n_m are defined as $\lambda_{p,q} = n_m D(p^2 + q^2)^{-1/2}$, where p and q are integers corresponding to diffraction order. We assume that nanoparticles are embedded in a homogeneous medium with $n_m = 1.5$. These kinds of structures can be fabricated by deposition of TiN nanoparticles onto the glass substrate and subsequently covering them with poly(methyl methacrylate) superstrate. The same approach was used to obtain Au and Al nanodisk arrays in a homogeneous environment.¹⁴ The symmetric surrounding is the key ingredient in this model, because the quality factor of a SLR sharply drops in the case of half-space geometry comprising substrate and superstrate with non-matching refractive indices.^{14,46,47} In all cases, nanostructures are illuminated from the top by plane wave with normal incidence along the z axis and polarization along the x or y axis. We calculate transmission T at the bottom of the structure and then characterize its spectral properties by $\sigma_{\text{ext}} = D^2(1 - T)$ in accordance with Refs. 4, 14, and 48. An adaptive mesh was used for an accurate description of the nanodisk shape. We apply periodic boundary conditions at the lateral boundaries of a unit cell (single nanodisk), while perfectly matched layer (PML) boundary conditions were used on the remaining top and bottom sides. Although the FDTD method is a comprehensive and well-established tool which shows excellent agreement with experimental results for SLRs,^{6,11,27} high- Q resonances with significant spatial extent (which is the case for SLRs⁵⁰) require its careful implementation. Extensive convergence tests for each set of parameters have been performed to avoid undesired reflections on the PMLs and overestimation of the SLR width.

Figures 3(a)–3(f) show that SLRs are easily tailored through the whole telecommunication wavelength range by varying lattice period D . It is highly important to choose the appropriate size of nanodisks: for fixed D , SLR becomes extremely narrow for $d = 160$ nm. For example, the SLR width at the L-band dramatically reduces to ≈ 1 nm, as shown in Fig. 3(a). Although it is clear that a further decrease in the nanodisk sizes leads to the increase in the Q -factor, we limit the discussion with the $d = 160$ nm value, because of extremely slow convergence of the FDTD method for such

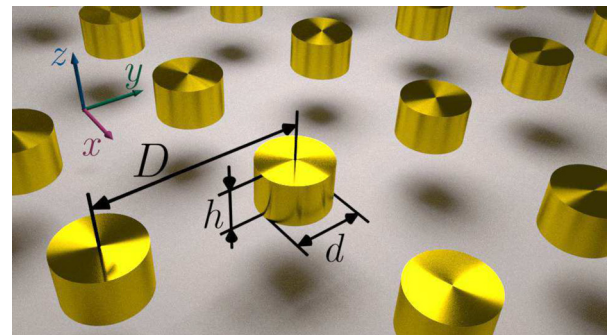


FIG. 2. The sketch of a system under consideration: $2D$ regular lattice with period D comprised of TiN nanodisks with height h and diameter d .

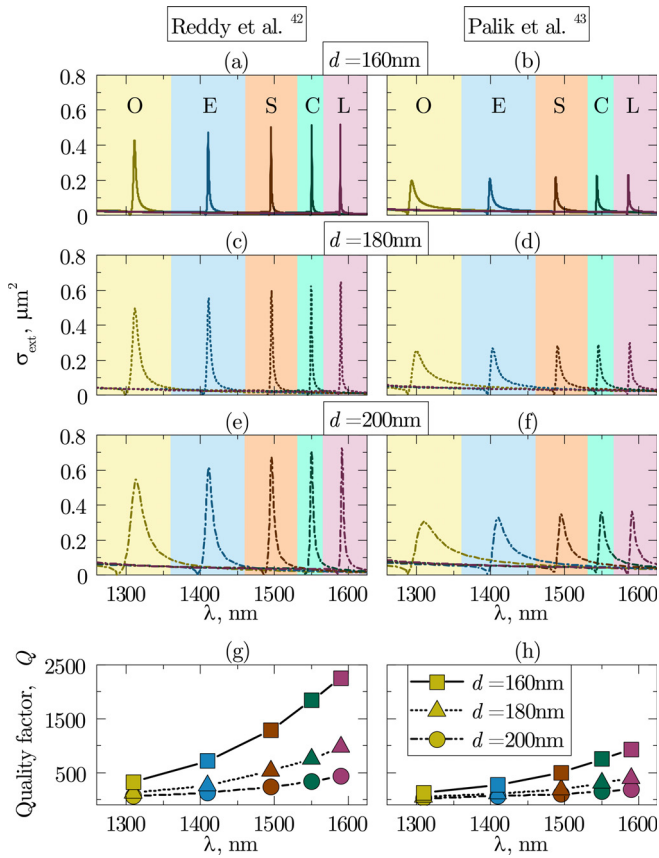


FIG. 3. (a)–(f) Extinction spectra (per particle) for 2D regular arrays from TiN nanodisks with various diameters d and heights $h = d/2$. Five different lattice periods D were chosen to generate SLRs at each telecommunication band: $D_O = 857$ nm, $D_E = 929$ nm, $D_S = 989$ nm, $D_C = 1026$ nm, $D_L = 1055$ nm; (g) and (h) Quality factors Q for corresponding peaks at: $\lambda_O = 1310$ nm, $\lambda_E = 1410$ nm, $\lambda_S = 1495$ nm, $\lambda_C = 1550$ nm, $\lambda_L = 1590$ nm. Two different datasets for ϵ of TiN are used in calculations: Refs. 42 (left panel) and 43 (right panel).

narrow-band resonances. In real experiment, Q would likely increase for $d < 160$ nm with fixed D ; however, at the same time, the position of the SLR peak may significantly depend on any imperfections: disorder of nanodisk positions or sizes. Thus, controlled generation of SLRs with a higher Q -factor becomes a complicated task. It can be also seen from Figs. 3(g) and 3(h) that for fixed nanodisk sizes, the quality factor Q gradually increases for larger values of D , which is consistent with the results from Ref. 14 for the visible range. For the most important telecommunication C-band, at $\lambda = 1550$ nm, the quality factor of SLR reaches the value of $Q \approx 1850$, which breaks the actual record $Q \approx 300$ for SLRs at the same wavelength.²⁷ It is also notable that quality factors of SLRs calculated with ϵ from Ref. 42 are about twice as much as the ones calculated for data from Ref. 43. Such a considerable difference in SLR Q -factors is expected, because ϵ of TiN thin films with thickness less than hundreds of nanometers significantly differs from ϵ of a bulk sample. Figures 3(g) and 3(h) show that appropriate tuning of TiN optical properties by varying its deposition conditions can significantly enhance SLRs in real experiment.

Finally, TiN, as a refractory plasmonic material, exhibits extraordinary stability at high temperatures³⁸ compared to conventional Au.⁵¹ Suppression of LSP resonance under aggressive conditions may totally deteriorate LSP-lattice hybridization;

therefore, the refractory behavior of TiN may become an additional advantage in the case of SLR generation at high temperatures. Figure 4 provides temperature-dependent SLR behavior at the most important telecommunication wavelength $\lambda = 1550$ nm. It can be seen that SLR is suppressed at high temperature, and the SLR peak position shifts by no more than $\Delta\lambda \approx 0.3$ nm at $T = 900^\circ\text{C}$ compared to the SLR peak at room temperature. Thus, the quality factor Q drops roughly 2 times, while the position of SLR is almost the same, which is significantly better than for conventional plasmonic materials, whose LSPs are almost suppressed⁵² at high temperatures. We note that experimental measurements of TiN dielectric permittivity in Ref. 42 imply that lattice dynamics, electron-phonon scattering, and other temperature-dependent phenomena are taken into account in $\epsilon(T)$. Therefore, FDTD simulations remain consistent, and additional consideration of these effects is not required.

Several possible issues related to experimental verification of obtained results are worth discussion. First, it is more possible to synthesize TiN nanopillars³⁷ in real experiment rather than nanodisks. However, it is easy to keep or even outperform reported values of Q by varying properly nanoparticle shapes and sizes. Second, it is quite difficult to perfectly match substrate and superstrate refractive indices, which obviously might significantly suppress SLRs. However, these complications are easily surpassed by generating parallel SLRs⁴⁹ or mimicking dipole resonances by excitation of monopoles above a mirror plane.⁵³ Both of these approaches exhibit greater tolerance to anti-symmetry of the surrounding medium refractive index. Finally, TiN dielectric permittivity ϵ in real experiment may significantly differ from datasets considered in this letter. Nevertheless, the reported results show that even TiN nanodisks with low- Q LSP (for ϵ taken from Ref. 43) exhibit high- Q SLRs (up to $Q = 1000$) for a particular set of geometric parameters. Thus, high- Q SLRs can be achieved in real experiment by careful choice of TiN deposition parameters and tuning its optical behavior for each particular case.

To conclude, we have shown that regular 2D arrays of TiN nanodisks are promising hybrid plasmonic systems which possess super-narrow high- Q SLRs within the whole telecommunication bandwidth. The quality factor and position of the SLR peak can be tailored through varying the lattice period D and sizes of nanoparticles. Refractory properties and large tunability of TiN optical properties make this material an attractive alternative to conventional Au and Ag which fail to tailor

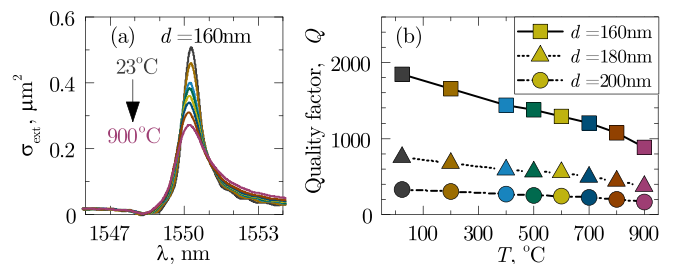


FIG. 4. (a) Temperature-dependent extinction spectra (per particle) and (b) corresponding quality factors Q for SLRs in 2D lattices of TiN nanodisks with fixed $D = 1026$ nm and for different diameters d and heights $h = d/2$. Temperature-dependent values of ϵ from Ref. 42 were used in simulations.

high- Q SLRs to telecom. Further development and extension of the reported approach open an opportunity to go beyond the telecommunication range and to increase the performance of SLRs in the IR region, which might be promising in mid-IR⁵⁴ and vibrational⁷ spectroscopies.

The authors thank Vadim Markel for careful reading and helpful feedback on the manuscript, Davy Gérard and Frédéric Laux for providing elaborative information on results reported in Ref. 14, and the anonymous reviewers for their helpful and constructive comments that greatly contributed to improving the final version of the paper.

This work was supported by the RF Ministry of Education and Science, the State contract with Siberian Federal University for scientific research in 2017–2019. Numerical calculations were performed using the MVS-1000M system at the Institute of Computational Modeling of the Siberian Branch of the Russian Academy of Sciences.

- ¹S. Zou, N. Janel, and G. C. Schatz, *J. Chem. Phys.* **120**, 10871 (2004).
- ²S. Zou and G. C. Schatz, *J. Chem. Phys.* **121**, 12606 (2004).
- ³V. A. Markel, *J. Phys. B: At., Mol. Opt. Phys.* **38**, L115 (2005).
- ⁴B. Auguie and W. L. Barnes, *Phys. Rev. Lett.* **101**, 143902 (2008).
- ⁵V. G. Kravets, F. Schedin, and A. N. Grigorenko, *Phys. Rev. Lett.* **101**, 087403 (2008).
- ⁶Y. Chu, E. Schonbrun, T. Yang, and K. B. Crozier, *Appl. Phys. Lett.* **93**, 181108 (2008).
- ⁷R. Adato, A. A. Yanik, J. J. Amsden, D. L. Kaplan, F. G. Omenetto, M. K. Hong, S. Erramilli, and H. Altug, *Proc. Natl. Acad. Sci.* **106**, 19227 (2009).
- ⁸Z. Li, S. Butun, and K. Aydin, *ACS Nano* **8**, 8242 (2014).
- ⁹B. D. Thackray, V. G. Kravets, F. Schedin, G. Auton, P. A. Thomas, and A. N. Grigorenko, *ACS Photonics* **1**, 1116 (2014).
- ¹⁰R. R. Gutha, S. M. Sadeghi, and W. J. Wing, *Appl. Phys. Lett.* **110**, 153103 (2017).
- ¹¹W. Zhou, M. Dridi, J. Y. Suh, C. H. Kim, D. T. Co, M. R. Wasielewski, G. C. Schatz, and T. W. Odom, *Nat. Nanotechnol.* **8**, 506 (2013).
- ¹²G. Vecchi, V. Giannini, and J. Gómez Rivas, *Phys. Rev. Lett.* **102**, 146807 (2009).
- ¹³F. Laux, N. Bonod, and D. Gérard, *J. Phys. Chem. C* **121**, 13280 (2017).
- ¹⁴D. Khlopin, F. Laux, W. P. Wardley, J. Martin, G. A. Wurtz, J. Plain, N. Bonod, A. V. Zayats, W. Dickson, and D. Gérard, *J. Opt. Soc. Am. B* **34**, 691 (2017).
- ¹⁵Z.-S. Zhang, Z.-J. Yang, J.-B. Li, Z.-H. Hao, and Q.-Q. Wang, *Appl. Phys. Lett.* **98**, 173111 (2011).
- ¹⁶L. Lin and Y. Yi, *Opt. Express* **23**, 130 (2015).
- ¹⁷A. D. Humphrey, N. Meinzer, T. A. Starkey, and W. L. Barnes, *ACS Photonics* **3**, 634 (2016).
- ¹⁸N. Mahi, G. Lévêque, O. Saison, J. Marae-Djoua, R. Caputo, A. Gontier, T. Maurer, P.-M. Adam, B. Bouhafs, and A. Akjouj, *J. Phys. Chem. C* **121**, 2388 (2017).
- ¹⁹T. V. Teperik and A. Degiron, *Phys. Rev. B* **86**, 245425 (2012).
- ²⁰L.-H. Du, J. Li, Q. Liu, J.-H. Zhao, and L.-G. Zhu, *Opt. Mater. Express* **7**, 1335 (2017).
- ²¹M. Hentschel, M. Saliba, R. Vogelgesang, H. Giessen, A. P. Alivisatos, and N. Liu, *Nano Lett.* **10**, 2721 (2010).
- ²²V. Grigoriev, S. Varault, G. Boudarham, B. Stout, J. Wenger, and N. Bonod, *Phys. Rev. A* **88**, 063805 (2013).
- ²³D. Wang, A. Yang, A. J. Hryn, G. C. Schatz, and T. W. Odom, *ACS Photonics* **2**, 1789 (2015).
- ²⁴R. Nicolas, G. Lévêque, J. Marae-Djoua, G. Montay, Y. Madi, J. Plain, Z. Herro, M. Kazan, P.-M. Adam, and T. Maurer, *Sci. Rep.* **5**, 14419 (2015).
- ²⁵R. Guo, T. K. Hakala, and P. Törmä, *Phys. Rev. B* **95**, 155423 (2017).
- ²⁶N. Kinsey, M. Ferrera, V. M. Shalaev, and A. Boltasseva, *J. Opt. Soc. Am. B* **32**, 121 (2015).
- ²⁷B. D. Thackray, P. A. Thomas, G. H. Auton, F. J. Rodriguez, O. P. Marshall, V. G. Kravets, and A. N. Grigorenko, *Nano Lett.* **15**, 3519 (2015).
- ²⁸P. A. Thomas, G. H. Auton, D. Kundys, A. N. Grigorenko, and V. G. Kravets, *Sci. Rep.* **7**, 45196 (2017).
- ²⁹G. V. Naik, V. M. Shalaev, and A. Boltasseva, *Adv. Mater.* **25**, 3264 (2013).
- ³⁰U. Guler, V. M. Shalaev, and A. Boltasseva, *Mater. Today* **18**, 227 (2015).
- ³¹A. Lalis, G. Tessier, J. Plain, and G. Baffou, *J. Phys. Chem. C* **119**, 25518 (2015).
- ³²A. Catellani and A. Calzolari, *Phys. Rev. B* **95**, 115145 (2017).
- ³³L. Gui, S. Bagheri, N. Strohhfeldt, M. Hentschel, C. M. Zgrabik, B. Metzger, H. Linnenbank, E. L. Hu, and H. Giessen, *Nano Lett.* **16**, 5708 (2016).
- ³⁴W. He, K. Ai, C. Jiang, Y. Li, X. Song, and L. Lu, *Biomaterials* **132**, 37 (2017).
- ³⁵R. Kamakura, S. Murai, S. Ishii, T. Nagao, K. Fujita, and K. Tanaka, *ACS Photonics* **4**, 815 (2017).
- ³⁶S. Bagheri, C. M. Zgrabik, T. Gissibl, A. Tittl, F. Sterl, R. Walter, S. D. Zuani, A. Berrier, T. Stauden, G. Richter, E. L. Hu, and H. Giessen, *Opt. Mater. Express* **5**, 2625 (2015).
- ³⁷J. A. Briggs, G. V. Naik, T. A. Petach, B. K. Baum, D. Goldhaber-Gordon, and J. A. Dionne, *Appl. Phys. Lett.* **108**, 051110 (2016).
- ³⁸U. Guler, J. C. Ndukaife, G. V. Naik, A. G. A. Nnanna, A. V. Kildishev, V. M. Shalaev, and A. Boltasseva, *Nano Lett.* **13**, 6078 (2013).
- ³⁹J. A. Briggs, G. V. Naik, Y. Zhao, T. A. Petach, K. Sahasrabudde, D. Goldhaber-Gordon, N. A. Melosh, and J. A. Dionne, *Appl. Phys. Lett.* **110**, 101901 (2017).
- ⁴⁰Y. Wang, A. Capretti, and L. Dal Negro, *Opt. Mater. Express* **5**, 2415 (2015).
- ⁴¹A. Perry and J. Schoenes, *Vacuum* **36**, 149 (1986).
- ⁴²H. Reddy, U. Guler, Z. Kudyshev, A. V. Kildishev, V. M. Shalaev, and A. Boltasseva, *ACS Photonics* **4**, 1413 (2017).
- ⁴³E. D. Palik, *Handbook of Optical Constants of Solids II* (Academic Press, New York, 1998), p. 1096.
- ⁴⁴Lumerical Solutions, FDTD Solutions, www.lumerical.com/tcad-products/fdtd/.
- ⁴⁵N. Bonod and J. Neauport, *Adv. Opt. Photonics* **8**, 156 (2016).
- ⁴⁶B. Auguie, X. M. Bendaña, W. L. Barnes, and F. J. García de Abajo, *Phys. Rev. B* **82**, 155447 (2010).
- ⁴⁷A. G. Nikitin, T. Nguyen, and H. Dallaporta, *Appl. Phys. Lett.* **102**, 221116 (2013).
- ⁴⁸A. I. Väkeväinen, R. J. Moerland, H. T. Rekola, A.-P. Eskelinen, J.-P. Martikainen, D.-H. Kim, and P. Törmä, *Nano Lett.* **14**, 1721 (2014).
- ⁴⁹A. Vitrey, L. Aigouy, P. Prieto, J. M. García-Martín, and M. U. González, *Nano Lett.* **14**, 2079 (2014).
- ⁵⁰A. Abass, S. R.-K. Rodriguez, J. Gómez Rivas, and B. Maes, *ACS Photonics* **1**, 61 (2014).
- ⁵¹H. Reddy, U. Guler, A. V. Kildishev, A. Boltasseva, and V. M. Shalaev, *Opt. Mater. Express* **6**, 2776 (2016).
- ⁵²V. S. Gerasimov, A. E. Ershov, S. V. Karpov, A. P. Gavriluk, V. I. Zakomirnyi, I. L. Rasskazov, H. Ågren, and S. P. Polyutov, *Opt. Mater. Express* **7**, 555 (2017).
- ⁵³S.-Q. Li, W. Zhou, D. Bruce Buchholz, J. B. Ketterson, L. E. Ocola, K. Sakoda, and R. P. H. Chang, *Appl. Phys. Lett.* **104**, 231101 (2014).
- ⁵⁴J.-N. Liu, M. V. Schulmerich, R. Bhargava, and B. T. Cunningham, *Opt. Express* **22**, 18142 (2014).